Journal of The Electrochemical Society, **156** (2) H123-H128 (2009)
0013-4651/2008/156(2)/H123/6/$23.00 © The Electrochemical Society

Behavior of Electrodeposited Cd and Pb Schottky Junctions on CH_3-Terminated n-Si(111) Surfaces

Stephen Maldonado and Nathan S. Lewis[*,z]

Beckman Institute and Kavli Nanoscience Institute, Division of Chemistry and Chemical Engineering, California Institute of Technology, Pasadena, California 91125, USA

n-Si/Cd and n-Si/Pb Schottky junctions have been prepared by electrodeposition of Cd or Pb from acidic aqueous solutions onto H-terminated and CH_3-terminated n-type Si(111) surfaces. For both nondegenerately (n-) and degenerately (n^+-) doped H–Si(111) electrodes, Cd and Pb were readily electroplated and oxidatively stripped, consistent with a small barrier height (Φ_b) at the Si/solution and the Si/metal junctions. Electrodeposition of Cd or Pb onto degenerately doped CH_3-terminated n^+-Si(111) electrodes occurred at the same potentials as Cd or Pd electrodeposition onto H-terminated n^+-Si(111). However, electrodeposition on nondegenerately doped CH_3-terminated n-Si(111) surfaces was significantly shifted to more negative applied potentials (by −130 and −347 mV, respectively), and the anodic stripping of the electrodeposited metals was severely attenuated, indicating large values of Φ_b for contacts on nondegenerately doped n-type CH_3–Si(111) surfaces. With either Cd or Pb, current–voltage measurements on the dry, electrodeposited Schottky junctions indicated that much larger values of Φ_b were obtained on CH_3-terminated n-Si(111) surfaces than on H-terminated n-Si(111) surfaces. Chronoamperometric data indicated that CH_3–Si(111) surfaces possessed an order-of-magnitude lower density of nucleation sites for metal electrodeposition than did H–Si(111) surfaces, attesting to the high degree of structural passivation afforded by the CH_3–Si surface modification.
 [DOI: 10.1149/1.3021450]

Manuscript submitted June 2, 2008; revised manuscript received October 13, 2008. Published December 9, 2008.

The interfacial properties of semiconductor electrodes can be controlled through deliberate chemical functionalization.[1-8] A two-step chlorination–alkylation reaction sequence has been shown to modify Si with covalently attached alkyl groups,[9] significantly reducing the rate of oxidation of Si in air while simultaneously producing a low density of interfacial electrical trap states at the Si surface.[9,10]

The presence of covalently bonded alkyl functionalities also introduces a surface dipole that shifts the energetics of the Si valence ($\mathbf{E}_{vb}$) and conduction ($\mathbf{E}_{cb}$) bandedges at the interface toward the energy of the vacuum level ($\mathbf{E}_{vac}$).[11] UV photoelectron spectroscopic data obtained under ultrahigh-vacuum conditions have indicated that the electron affinity (χ) (the energy difference from $\mathbf{E}_{cb}$ to $\mathbf{E}_{vac}$) is ~0.5 eV less for CH_3–Si(111) surfaces than for H–Si(111) surfaces.[12] For an ideal contact between an n-type semiconductor and another conductive phase (e.g., a metal, a conductive polymer, or a solution with a dissolved redox couple), the equilibrium junction barrier height, Φ_b, is given by

$$-q\Phi_b = \mathbf{E}_F + \chi \quad [1]$$

where q is the unsigned elementary electronic charge, $\mathbf{E}_F$ is the Fermi level of the conductive phase, and more negative energies are further from the vacuum level. Hence, the change in χ produced by alkylation should produce different barrier heights for ideal semiconductor/metal Schottky barriers on H–Si(111) and CH_3–Si(111) surfaces.

For Si(111)/Hg Schottky junctions, the measured differences in Φ_b between H-terminated and CH_3-terminated Si(111) are in excellent agreement with the change in χ measured upon alkylation.[13] The ideal behavior of the Hg junctions likely arises from the "soft" nature of Hg contacts to Si, because Hg-silicide does not form at ambient conditions and Hg does not react with the Si–C surface bonds.[14-16] In contrast, Schottky barriers produced by thermal evaporation of Cu, Au, and Ag onto CH_3–Si(111) do not exhibit the expected increase in barrier height relative to Schottky barriers produced by evaporation of these metals onto H–Si(111) surfaces.[17] This behavior likely reflects the propensity of evaporated transition metals to form interfacial silicides[14] or to disrupt the CH_3–Si surface layer.

Extension of the Si/Hg results to other metals thus requires soft methods for deposition of metal contacts onto Si surfaces. Electrodeposition has been used extensively to form microscale and macroscale metal/semiconductor contacts[18-30] as well as to deposit metal-catalyst islands onto semiconductor photoelectrodes.[25,31-35] An attractive feature of electrodeposition relative to other metal-deposition techniques is that the process can be monitored in situ while providing qualitative and quantitative information on the energetics and physical state of the semiconductor surface.[18,29,30,36,37]

We report herein the electrodeposition of Cd and Pb films onto H- and CH_3-terminated n-Si(111). Neither Cd nor Pb readily forms silicides at ambient temperature and pressure,[14] so these metals provide interesting systems to evaluate whether electrodeposited metal contacts can yield the expected variation in barrier height as the dipole of the Si(111) surface is changed by alkylation. The electrochemical responses, and corresponding solid-state electrical junction data, of electrodeposited Cd and Pb junctions using degenerately doped and nondegenerately doped n-type H–Si(111) and CH_3–Si(111) surfaces have been investigated to determine whether CH_3 monolayers predictably and consistently influence the electrochemical and electrical properties of Si interfaces. In addition, chronoamperometric data have been used to compare the available nucleation-site density for metal electrodeposition onto CH_3–Si(111) and H–Si(111) surfaces, allowing an investigation of whether these different surface functionalities can effect different metal-plating properties on Si surfaces.

Experimental

Materials.— Single-side polished, nondegenerately phosphorus-doped (n-type), 525 μm thick Si(111) wafers, with miscut angles ±0.5° and resistivities between 1 and 10 Ω cm, were purchased from ITME (Warsaw, Poland). Double-side polished, degenerately phosphorus-doped (n^+), 300 μm thick silicon wafers, with miscut angles ±0.5° and nominal resistivities of ≤0.004 Ω cm, were obtained from Addison Engineering, Inc. (San Jose, California). Prior to chemical treatment, the specific resistivity of each wafer was determined using four-point-probe methods. Replicate measurements were conducted using Si samples cut from the same parent wafer.

All chemicals used for silicon cleaning, silicon surface functionalization, and electrochemical analyses were used as received. Water with a resistivity >18 MΩ cm was obtained from a Barnstead Nanopure system and was used throughout.

* Electrochemical Society Active Member.
z E-mail: nslewis@its.caltech.edu

Si surface functionalization.— Before surface functionalization, silicon wafers were sectioned into 1 × 5 cm pieces that were degreased by sequentially immersing and sonicating in methanol (Aldrich), acetone (Aldrich), 1,1,1-trichloroethane (Aldrich), dichloromethane (Fisher), 1,1,1-trichloroethane, acetone, and methanol for 5 min each. The Si pieces were then immersed in a 3:1 (by volume) solution of 18 M H_2SO_4 (Fisher) and 30% H_2O_2(aq) (v/v, Fisher) at ~80° for ≥1 h, followed by a rinse with H_2O. H-terminated Si(111) surfaces were prepared by immersion of these Si samples for 10 min in 11 M NH_4F(aq) (Transene),[38-42] with periodic agitation to minimize accumulation of bubbles at the surface. The Si samples were then rinsed thoroughly with water and were used immediately for further chemical functionalization or for electrochemical analysis. The samples that were used for electrochemical measurements without further functionalization were contacted with In–Ga eutectic on the back side prior to etching the top surface.

CH_3-terminated Si(111) surfaces were prepared as described previously.[13,43] First, freshly H-terminated Si(111) surfaces were chlorinated by immersion for 50 min at 90°C into a saturated PCl_5 (Aldrich) solution in chlorobenzene (Aldrich). The chlorine-terminated Si(111) samples were then rinsed sequentially with chlorobenzene and tetrahydrofuran (THF, Aldrich), followed by immersion for 8–12 h at 70°C in a 1 M CH_3MgBr solution in THF. The CH_3-terminated Si(111) surfaces were then rinsed with THF, rinsed with methanol, and sonicated sequentially in methanol, acetone, and methanol for 5 min each. The samples were then rinsed with water and dried under a stream of N_2(g).

Electrochemical metal deposition and solid-state device measurements.— After chemical treatment, the n-Si(111) samples were diced into 1 × 1 cm pieces. To make ohmic contacts to these Si samples, the back side was lightly scratched with a diamond scribe, etched for 10 min with 11 M NH_4F(aq), and then rubbed with a Ga–In eutectic. The Si samples were then placed on a 1 × 2.5 × 0.2 cm stainless steel support and were fitted onto a stainless steel base plate. A Teflon cell with a 0.2 cm diameter Viton O-ring was then press-fit on top of the Si sample, exposing a surface area of 0.128 cm^2.[13]

For full metal-film preparation, a two-step nucleation-growth chronoamperometric protocol was used.[44] A standard three-electrode setup with a reference and a Pt mesh counter electrode was used. Solutions for Cd electrodeposition consisted of 5 mM $CdSO_4$ (Fisher) dissolved in 0.1 M H_2SO_4(aq) (Fisher). Pb electrodeposition solutions contained 5 mM $Pb(ClO_4)_2$ (Aldrich) in 0.1 M $HClO_4$(aq) (Fisher).

Metal-film electrodeposition was performed using a combination of potential steps at high overpotentials, followed by steps to low overpotentials to generate finely sized and spaced metal nuclei[45-47] and to subsequently produce even film growth between metal clusters.[48] For Cd electrodeposition on H-terminated n-Si(111), and for both types of n^+-Si(111) electrode samples, a series of ten 100 ms steps, from open circuit to −0.90 V vs a saturated calomel electrode (SCE), were applied, followed by a 10 min step at −0.75 V vs SCE. The open-circuit potentials (OCPs) were −0.10 ± 0.08 and −0.2 ± 0.2 V vs SCE for H-terminated n-Si(111) and n^+-Si(111) electrodes, respectively. The OCP for CH_3-terminated n^+-Si(111) was 0.17 ± 0.02 V vs SCE. For Cd-film electrodeposition on CH_3-terminated n-Si(111), thirty 100 ms potential steps, from open circuit (−0.05 ± 0.04 V) to − 1.0 V vs SCE, were used, followed by a single 10 min step at −0.90 V vs SCE. For Pb electrodeposition on H-terminated n-Si(111), and for both n^+-Si(111) surfaces, ten 100 ms potential steps, from open circuit to −0.60 V vs SCE, were applied, followed by a 10 min step at −0.55 V vs SCE. The OCPs for H-terminated n-Si(111) and n^+-Si(111) electrodes were −0.09 ± 0.04 and −0.22 ± 0.02 V vs SCE, respectively, and was 0.1 ± 0.1 V vs SCE for CH_3-terminated n^+-Si(111). For CH_3-terminated n-Si(111) electrodes, thirty 100 ms potential steps from open circuit (−0.1 ± 0.1 V) to − 0.95 V vs SCE were used, with a subsequent 10 min potential step at −0.88 V vs SCE.

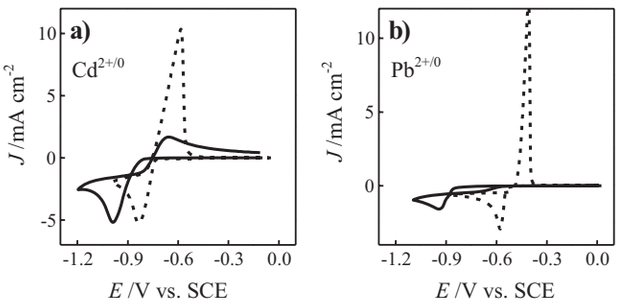

Figure 1. Representative cyclic voltammograms of (dashed) H-terminated and (solid) CH_3-terminated nondegenerately doped n-Si(111) electrodes immersed in deaerated aqueous acidic solutions: (a) *J-E* data for electrodeposition of Cd from a 0.1 M H_2SO_4 solution containing 0.005 M $CdSO_4$ and (b) *J-E* data for electrodeposition of Pb from a 0.1 M $HClO_4$ solution containing 0.005 M $Pb(ClO_4)_2$. Scan rate: 0.030 V s^{-1}

All voltammetry and chronoamperometry data were collected with the electrodes in the dark, in deaerated solutions, with scans initiated at the OCP of the working electrode. For electrochemical current density–potential (*J-E*) data, cathodic (reducing) and anodic (oxidizing) currents are plotted as negative and positive, respectively. For steady-state electrical current density–voltage (*J-V*) data, forward-bias voltages and currents are plotted as positive. Voltammetric data were obtained using a Solartron Instruments potentiostat (SI1287) interfaced to a computer for data acquisition. All reported cyclic voltammetric data were recorded at a scan rate of 0.030 V s^{-1} and were averages of separate measurements on at least five different samples. Chronoamperometry was performed with a Princeton Applied Research (PAR) model 362 potentiostat coupled to a PAR model 175 universal programmer. Data were collected with a Tektronix TK200 digital oscilloscope that was interfaced to a data-acquisition computer. A spring-loaded brass top contact was used to make electrical connection to the deposited metal film for solid-state *J-V* measurements.

Characterization.— X-ray photoelectron spectroscopic (XPS) data were obtained using an M-Probe spectrometer equipped with a 1486.6 eV Al Kα X-ray source.[49] The pressure during data collection was ≤5 × 10^{-9} Torr, and data were obtained using an incident angle of 35° off of the surface normal. For all samples, Si 2p spectra were obtained in the 106–96 eV energy region. All spectra were averaged over 30 scans that were obtained with a spot diameter of 300 μm and a resolution of 0.6 eV. Following the nucleation step, metallized Si samples were immediately loaded into the spectrometer, and scans were acquired after the base pressure had been obtained.

Results

Voltammetric responses of n-type Si(111) in aqueous Cd^{2+} and Pb^{2+} solutions.— Figure 1 displays representative *J-E* data for n-Si(111) working electrodes immersed in aqueous acidic solutions that contained either dissolved Cd^{2+} or Pb^{2+}. In accord with previous reports, reversible Cd or Pb metal reduction and metal oxidation (stripping) was observed for freshly etched, H-terminated, n-Si(111) electrodes (Fig. 1a and b).[26-29] The ratios of the anodic to cathodic charge density (Q_a/Q_c) passed in the voltammograms in Fig. 1a and b for H-terminated n-Si(111) were near unity (Table I), indicating that these Si/metal junctions were not strongly rectifying, i.e., anodic and cathodic current densities ≫1 mA cm^{-2} in magnitude were observed at positive and negative potentials, respectively, under these experimental conditions.

Table I. Voltammetric responses for metal electrodeposition on n-type Si(111).[a]

Metal	Surface functionalization	$E_{p,c}$ (V vs SCE)	$\lvert\Delta E_{p,c}\rvert$ (V)[b]	$E_{p,a}$ (V vs SCE)	$\lvert\Delta E_{p,a}\rvert$ (V)[c]	Q_a/Q_c[d]	N_D (cm^{-3})[e]	$q\Phi_{JV}$ (eV)[f]
Cd								
	Nondegenerate doping							
	–H	−0.833 ± 0.003		−0.586 ± 0.012		0.90 ± 0.03	$(3 \pm 2) \times 10^{15}$	⩽0.4
	$-CH_3$	−0.964 ± 0.017		−0.656 ± 0.008		0.31 ± 0.04	$(1.5 \pm 0.3) \times 10^{15}$	0.81 ± 0.05
			0.131 ± 0.017		0.070 ± 0.014			
	Degenerate doping							
	–H	−0.827 ± 0.004		−0.585 ± 0.003		0.962 ± 0.007	$(3.4 \pm 0.5) \times 10^{19}$	—
	$-CH_3$	−0.827 ± 0.007		−0.581 ± 0.004		0.966 ± 0.006	$(3.4 \pm 0.5) \times 10^{19}$	—
			0.000 ± 0.008		0.004 ± 0.005			
Pb								
	Nondegenerate doping							
	–H	−0.577 ± 0.010		−0.408 ± 0.003		0.84 ± 0.02	$(2 \pm 1) \times 10^{15}$	⩽0.59
	$-CH_3$	−0.924 ± 0.031		—		0.02 ± 0.01	$(1.3 \pm 0.9) \times 10^{15}$	0.82 ± 0.03
			0.347 ± 0.024		—			
	Degenerate doping							
	–H	−0.577 ± 0.014		−0.410 ± 0.005		0.91 ± 0.03	$(3.4 \pm 0.5) \times 10^{19}$	—
	$-CH_3$	−0.583 ± 0.026		−0.401 ± 0.005		0.90 ± 0.02	$(3.4 \pm 0.5) \times 10^{19}$	—
			0.006 ± 0.030		0.009 ± 0.007			

[a] $T = 295 \pm 3$ K; 1 scan at 0.030 V s^{-1}; the averages and standard deviations were determined from five separate samples for each condition.
[b] $\lvert\Delta E_{p,c}\rvert = \lvert E_{p,c,Si-H} - E_{p,c,Si-CH_3}\rvert$.
[c] $\lvert\Delta E_{p,a}\rvert = \lvert E_{p,a,Si-H} - E_{p,a,Si-CH_3}\rvert$.
[d] Q_c = integrated cathodic (metal deposition) charge density passed; Q_a = integrated anodic (stripping) charge density passed.
[e] Measured by four-point probe.
[f] Measured from dark *J-V* responses of electrochemically deposited dry device.

Essentially, identical behavior was observed when the dopant density of the H-terminated n-type Si(111) electrodes was increased from 10^{15} to 10^{19} cm^{-3} (Fig. 2). The Q_a/Q_c ratios were only slightly larger for H-terminated n^+-Si(111) electrodes than for H-terminated n-Si(111) electrodes (Table I). The cathodic and anodic peak potentials ($E_{p,c}$ and $E_{p,a}$, respectively) for Cd^{2+} or Pb^{2+} electrodeposition were statistically indistinguishable between nondegenerately doped and degenerately doped H-terminated Si(111) electrodes (Table I). The close similarity between the data for nondegenerately doped and degenerately doped H-terminated Si(111) indicates that the observed electrodeposition overpotentials are not dominated by the presence of a significant built-in voltage (V_{bi}) in the H-terminated n-Si(111) electrodes.

In contrast, significant differences were observed between the voltammetry of Cd^{2+} or Pb^{2+} at CH_3- and H-terminated n-Si(111) electrodes (Fig. 1). The voltammetric wave shapes and peak heights observed with CH_3-terminated n-Si(111) electrodes were less reversible in both reduction and oxidation than with H-terminated n-Si(111) electrodes. For Cd electrodeposition at 0.030 V s^{-1}, changing from H- to CH_3-terminated n-Si(111) produced a shift in $E_{p,c}$ of -0.131 ± 0.007 V (Fig. 1a), while for Pb electrodeposition the value of $E_{p,c}$ shifted by -0.347 ± 0.024 V (Fig. 1b). In addition, a greater extent of "crossover" was observed between the forward and reverse scans[37,50] on CH_3-terminated n-Si(111) than on H-terminated n-Si(111). Also, the anodic currents on the oxidative scan were suppressed on CH_3-terminated n-Si(111) for both Cd^{2+} and Pb^{2+}, with Q_a/Q_c values much smaller than unity for Cd^{2+} and nearly 0 for Pb^{2+} (Fig. 1, Table I). For oxidative stripping of Cd, changing from H–Si(111) to CH_3–Si(111) electrodes produced a shift in $E_{p,a}$ of -0.070 ± 0.014 V, whereas no anodic voltammetric wave for Pb oxidative stripping was observed with CH_3-terminated n-Si(111) electrodes.

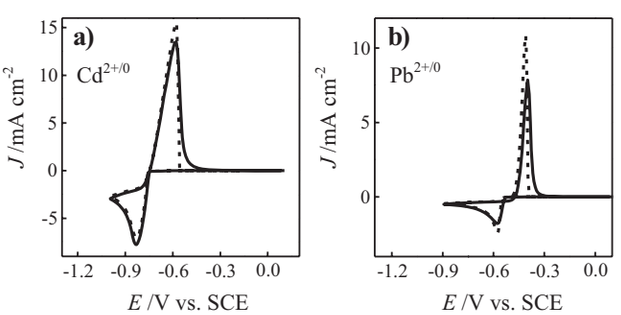

Figure 2. Representative cyclic voltammograms of (dashed) H-terminated and (solid) CH_3-terminated degenerately doped n^+-Si(111) electrodes immersed in deaerated aqueous acidic solutions: (a) *J-E* data for electrodeposition of Cd from a 0.1 M H_2SO_4 solution containing 0.005 M $CdSO_4$ and (b) *J-E* data for electrodeposition of Pb from a 0.1 M $HClO_4$ solution containing 0.005 M $Pb(ClO_4)_2$. Scan rate: 0.030 V s^{-1}

Unlike the situation for H-terminated Si(111) surfaces, the voltammetric behavior of CH_3-terminated n-type Si(111) was strongly influenced by the dopant density, N_D. In fact, the voltammetric responses of CH_3-terminated n^+-Si(111) electrodes closely resembled those of H-terminated Si(111) (Fig. 2). The values of Q_a/Q_c, $E_{p,c}$, and $E_{p,a}$ for Cd and Pb electrodeposition did not differ statistically between CH_3-terminated and H-terminated n^+-Si(111) electrodes (Fig. 2, Table I). The CH_3-terminated n^+-Si(111) electrodes exhibited clear and narrow stripping peaks on the back scan, with values of $Q_a/Q_c \approx 1.0$ within this potential range.

The change in the voltammetry of CH_3-terminated Si(111) electrodes in response to a change in the bulk doping density implies that a significant built-in voltage within the near-surface region of the Si contributed to the electrodeposition/oxidation overpotentials observed for CH_3-terminated n-Si(111) electrodes. The contribution of V_{bi} to the required electrodeposition overpotential is minimized at n^+-Si(111) electrodes, because the depletion-layer width is sufficiently thin ($\sim 10^{-9}$ m for $\Phi_b = 1$ V for Si with $N_D = 10^{19}$ cm^{-3})[51] that large tunneling currents of electrons from the bulk semiconductor through the depletion region into solution are possible.[37,52] The similarity of the values of $E_{p,c}$ and $E_{p,a}$ for CH_3-terminated and H-terminated n^+-Si(111) electrodes further indicates that charge

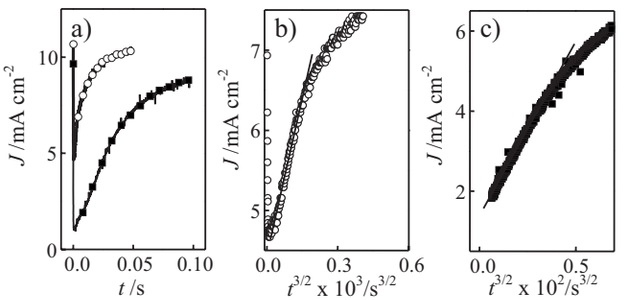

Figure 3. Potentiostatic pulse deposition of Cd nuclei at −0.9 V vs SCE in deaerated 0.1 M H_2SO_4 with 0.005 M $CdSO_4$: (a) *J-t* responses for (open circles) H-terminated and (closed squares) CH_3-terminated n^+-Si(111) electrodes, (b) $J\text{-}t^{3/2}$ response for H-terminated n^+-Si(111), and (c) $J\text{-}t^{3/2}$ response for CH_3-terminated n^+-Si(111). The *y* axes for (b) and (c) have been chosen to emphasize the linear region used for analysis, as described in the text.

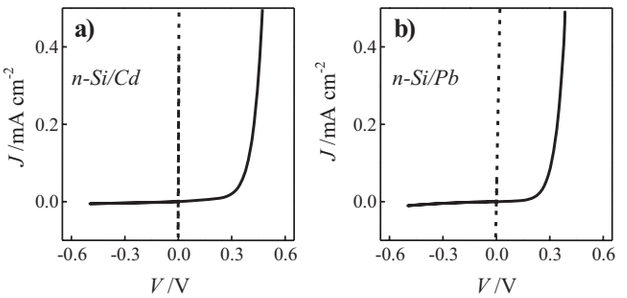

Figure 4. Representative electrical responses of electrodeposited metal/n-Si(111) Schottky junctions: (a) *J-V* data for Cd Schottky junctions with (dashed) H-terminated and (solid) CH_3-terminated n-Si(111), where $T = 296 \pm 2$ K, and (b) *J-V* data for Pb Schottky junctions with (dashed) H-terminated and (solid) CH_3-terminated n-Si(111), where $T = 296 \pm 2$ K. Film thicknesses were approximately 200 nm.

transfer is not substantially (i.e., by >6 mV overpotential) impeded by through-bond tunneling through the surface passivation layer.[53]

Chronoamperometric deposition of Cd onto H-terminated and CH_3-terminated n^+-Si(111).— Continuous metal films were more readily deposited on H-Si(111) than on CH_3-Si(111) surfaces. This effect was investigated quantitatively by measurement of the transient currents for the first nucleation step on H- and CH_3-terminated n^+-Si(111) working electrodes. At an overpotential of ~150 mV and long times, the total charge passed was essentially the same at both electrode types. In contrast, the initial current density–time (*J-t*) responses at this overpotential differed significantly. Figure 3 depicts representative chronoamperometric data at short times for the initial Cd nucleation step for both H- and CH_3-terminated n^+-Si(111) electrodes biased at −0.90 V vs SCE, with the H-terminated n^+-Si(111) samples exhibiting larger initial transient currents. Following the analysis of Hills et al.,[54] the currents recorded at early times provide mechanistic information on the metal-nucleation process. For an electrode held at a constant potential, progressive nucleation, in which the number of nucleation events increases with time (t), is indicated if J is linear with $t^{3/2}$[37,54]

$$J(t) = \frac{zN_\infty\pi(2D_{Cd^{2+}}C_{Cd^{2+}})^{3/2}M_{Cd^{2+}}^{1/2}t^{3/2}}{3\rho_{Cd}^{1/2}} \quad [2]$$

where n is the number of electrons transferred, $D_{Cd^{2+}}$ is the diffusion coefficient of Cd^{2+} in solution ($cm^2\ s^{-1}$), $C_{Cd^{2+}}$ is the solution concentration of Cd^{2+} (moles cm^{-3}), $M_{Cd^{2+}}$ is the atomic mass of Cd ($g\ mol^{-1}$), ρ_{Cd} is the density of Cd ($g\ cm^{-3}$), and N_∞ is the nucleation density (cm^{-2}) of Cd at infinite time. Figures 3b and c explicitly depict the early-time, linear dependence of J with $t^{3/2}$ for the H- and CH_3-terminated n^+-Si(111) electrodes of Fig. 3a. From the slopes of the linear fits in Fig. 3b and c, the values of N_∞ for H-terminated Si(111) and CH_3-terminated Si(111) surfaces were determined to be $(1.1 \pm 0.2) \times 10^9\ cm^{-2}$ and $(0.13 \pm 0.05) \times 10^9\ cm^{-2}$, respectively.

For electrodeposition of Au or Ag on freshly etched single-crystalline Si, values of N_∞ at mild overpotentials (<200 mV), where diffusion of electroactive species is not the dominating process in nucleation, have been reported to be between 10^9 and $10^{11}\ cm^{-2}$.[18,19,44,55] These N_∞ values are in agreement with the data observed herein for deposition of Cd or Pb on H-terminated n^+-Si(111). In contrast, the total apparent number of existing nucleating sites for a one-pulse electrodeposition experiment of Cd or Pb on CH_3-terminated Si(111) was approximately an order of magnitude smaller than that for 11 M NH_4F(aq) etched n^+-Si(111) electrodes.

Electrical properties of electrochemically deposited n-Si(111)/Cd and n-Si(111)/Pb Schottky junctions.— Figure 4 depicts the electrical properties of electrodeposited n-Si/Cd and n-Si/Pb Schottky junctions. At room temperature, the junctions with CH_3-terminated n-Si(111) were considerably more rectifying than the junctions with H-terminated n-Si(111) (Fig. 4a and b). The values of Φ_b for the Cd and Pb Schottky devices with CH_3-Si(111) surfaces were 0.81 and 0.82 ± 0.03 V, respectively, as determined from the dark *J-V* data (Table I). In contrast, the H-terminated n-Si(111) substrates exhibited much lower barrier heights, with Cd and Pb junctions exhibiting Φ_b <0.4 and <0.59 V, respectively. For these junctions, the *J-V* responses were not sufficiently rectifying at room temperature to allow unambiguous determination of Φ_b from the *J-V* data.[13] A small fraction of the tested H-terminated n-Si(111)/Pb devices exhibited values of Φ_b as large as 0.59 V, but the majority of the H-terminated n-Si(111)/Pb junctions showed poor or no rectification, consistent with previous reports.[56] Hence, the values for electrochemically prepared H-terminated n-Si(111) devices are reported as upper estimates of Φ_b. For all junctions that exhibited rectification, the overall diode quality factors ranged between 1.8 and 2.

X-ray photoelectron spectra of Si(111) surfaces after electrodeposition of Cd and Pb.— Figure 5 displays representative high-resolution Si 2p XPS data for H- and CH_3-terminated n-Si(111)

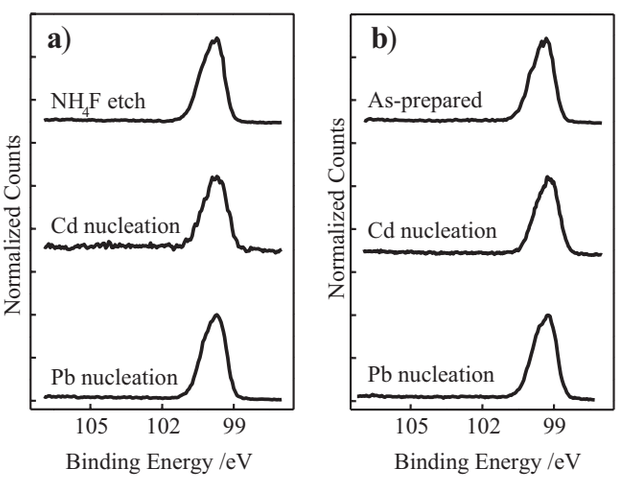

Figure 5. X-ray photoelectron spectra of the Si 2p region of (a) H-terminated and (b) CH_3-terminated n-Si(111) electrode surfaces (top) as-prepared, (middle) after initial Cd nucleation step, and (bottom) after initial Pb nucleation step.

electrodes after the initial metal nucleation step during the deposition of Cd or Pb films. No oxide signatures were apparent between 101 and 105 eV for any of the analyzed surfaces. For both H- and CH_3-terminated n-Si(111) surfaces, these results suggest that neither Cd nor Pb electrodeposition resulted in interfacial silicon oxide thicknesses $\geqslant 1$ Å.

Discussion

Influence of surficial CH_3-groups on the barrier height of Si/Cd and Si/Pb Schottky junctions.— The electrochemical and electrical data support the expectation that the presence of a surface dipole arising from the attachment of CH_3- groups to Si(111) surfaces will substantially (i.e., by ~ 0.5 V) shift the bandedges closer to the vacuum level as compared to the H-terminated Si(111) surface.[11-13,57] The net change in the value of χ at the Si(111) interface is manifest in the increased junction barrier heights for the investigated CH_3-terminated Si(111)/metal and Si(111)/solution junctions. The *J-V* properties of the electrodeposited dry n-Si(111)/Cd and n-Si(111)/Pb Schottky junctions were ohmic for H-terminated n-Si(111), while these same junctions were strongly rectifying with CH_3-terminated Si(111). These Cd and Pb Schottky junctions prepared by electrodeposition displayed electrical properties that are in agreement with the previously reported *J-V* responses of n-Si(111)/Hg junctions[13] and support the hypothesis that Schottky junctions prepared by thermal metal evaporation do not reflect the innate properties of the CH_3-terminated Si interfaces because of physical damage or chemical reactivity during the deposition process.

The voltammetric data of the n-type Si electrodes in contact with the metal plating solutions further illustrate the differences in surface energetics of CH_3-terminated and H-terminated Si(111). The close correspondence between the charge density passed in the forward and reverse sweeps of the voltammograms in Fig. 2 for H-terminated Si(111) is consistent with the hypothesis that these Si electrodes are not strongly depleted[48] during Cd and Pb electrodeposition, i.e., the H-terminated n-Si(111) interface is not strongly rectifying toward reduction/oxidation of either $Cd^{2+/0}$ or $Pb^{2+/0}$. In acidic (non-HF containing) aqueous solutions, the potential of the conduction bandedge, $\mathbf{E}_{cb}$, of H-terminated Si(111) has been estimated as -0.50 ± 0.05 V vs SCE.[58] The potentials of $Cd^{2+/0}$ and $Pb^{2+/0}$ electrodeposition (-0.74 and -0.52 V vs SCE, respectively)[28,29] are near, or more negative than, the conduction bandedge of H-terminated n-Si(111), so a depletion region in n-Si(111) is not expected during the electroreduction of these metals. The identical features of the voltammetric responses displayed for H-terminated n-Si(111) and n^+-Si(111) electrodes support this premise, with the surface energetics and V_{bi} having minimal influence on the interfacial charge transfer at degenerately doped semiconductor electrodes.[52]

In contrast, the voltammetric responses indicate that CH_3-terminated n-Si(111) electrodes are largely depleted of majority carriers during the electrodeposition of Cd or Pb. The susceptibility of CH_3-terminated Si(111) surfaces to electrochemical oxidation at potentials >0.3 V vs SCE[59] precluded direct measurement of E_{cb} and Φ_b by standard impedance methods. However, examination of the *J-E* behavior of CH_3-terminated n-Si(111) electrodes in aqueous solutions containing dissolved methyl viologen has demonstrated that the bandedges of CH_3-terminated Si(111) are invariant to changes in solution pH and in acidic solutions are situated at significantly (i.e., 0.3–0.4 V) more negative potentials than the bandedges of freshly etched n-Si(111).[11] The electrochemical behavior of CH_3-terminated n^+-Si(111) is expected to more closely approximate that of H-terminated Si(111) electrodes, if the additional electrodeposition overpotentials arise largely from V_{bi}. Comparison of Fig. 1 and 2 indeed shows a significant difference in the voltammetric behavior of CH_3-terminated Si(111) electrodes as the bulk Si donor density is varied, consistent with the hypothesis that CH_3-terminated n-Si(111) surfaces are in depletion for the electrodeposition of Cd and Pb under our experimental conditions.

The data depicted in Fig. 2 argue against the plausibility of through-bond tunneling across the CH_3 groups as a significant factor in the differences observed between metal electrodeposition at CH_3- and H-terminated n-type Si(111) electrodes. On Au(111) electrodes, Schneeweiss et al. have shown that butanethiol, pentanethiol, and hexanethiol monolayers can act as large electron tunneling barriers that slow the overall rate of Cu electrodeposition at low overpotentials. These insulating monolayers effected >200 mV shifts in the peak potential of the cyclic voltammetry of Cu electrodeposition.[53] For comparison, with electrodeposition of Cd and Pb, respectively, onto Si (Fig. 2), the values of $E_{p,c}$ and $E_{p,a}$ were not statistically different between the two n^+-Si(111) electrode types. These data suggest similar metal electrodeposition charge-transfer rate constants for these H- and CH_3-terminated Si surfaces. For nondegenerately doped semiconductor electrodes, evaluation of explicit charge-transfer kinetics from descriptive cylic voltammetric features such as ΔE_p is not straightforward, because the *J-E* responses of semiconductor electrodes are sensitive to the standard rate constant of the charge-transfer process and to the potential dependence of the population of transferable electrons at the interface.[52,60-63] For metal electrodeposition/oxidation, the determination of interfacial charge-transfer rate constants is further complicated by the spatial dispersion of deposited metal nuclei, the magnitude of current flow at the metal/semiconductor contacts, and the complex, multicharge-transfer step mechanisms.[29,30,48,64] Accordingly, the data presented herein do not allow for direct comparison of explicit charge-transfer rate constants at H- and CH_3-terminated Si(111) electrodes. Nevertheless, the similarities between the electrodeposition behavior for both Cd and Pb onto degenerately doped CH_3-terminated n^+-Si(111) indicates that through-bond electron tunneling is not a dominant factor in these electrodeposition processes at CH_3-terminated n-Si(111) electrodes.

The electrical and electrochemical data were also not influenced significantly by insulating interfacial silicon oxide layers. Although oxidation of Si interfaces immersed in aqueous electrolytes at pH 1 is thermodynamically favored at potentials $\geqslant -1.1$ V vs Ag/AgCl,[58] the data in Fig. 5 suggest that the formation of a multilayer oxide on n-Si in deaerated acidic solutions, biased cathodically and in the absence of illumination, is kinetically slow on the timescale of the deposition experiments. Unlike aqueous acidic Au^{3+} or Ag^+ solutions, which readily oxidize Si surfaces, solutions of dissolved Cd^{2+} or Pb^{2+} apparently do not have sufficient oxidizing power to form appreciable SiO_x layers on either CH_3- or H-terminated Si.[27,58] Hence, under the conditions employed herein, the electrochemical and electrical properties of the Si/metal interfaces reflect the native surface chemistries of CH_3- and H-terminated Si(111).

Chemical passivation of Si by CH_3 surface groups.— Chemical modification of Si(111) surfaces by the chlorination/Grignard alkylation method results in an essentially complete, protective layer attached to the topmost Si atoms. Scanning tunneling microscopy of CH_3-terminated Si(111) surfaces has revealed a low density of defects in the monolayer coverage of chemically grafted CH_3 groups.[65] Transient photoconductivity measurements have also demonstrated that CH_3-terminated Si(111) surfaces possess an unusually low density of electrically active surface trap states.[10] The lower measured value of N_∞ for CH_3-terminated Si(111) surfaces relative to NH_4-etched Si(111) surfaces is in qualitative agreement with these prior observations. Direct comparisons between the areal densities of nucleation sites and electrical trap states are confounded by the well-known difficulties in precisely assessing the nucleation site density solely from electrochemical data.[37,66] Nevertheless, because electrodeposition of metal films occurs by metal cluster nucleation at individual high-energy surface sites that then grow larger and fuse together,[67-69] the observation of hindered film growth on CH_3-terminated Si(111) agrees with expectations and with the chronoamperometric data. From a practical standpoint, a decrease in the available nucleation site density on Si(111) as a result of the intro-

duction of surficial CH_3 groups implies possible difficulty with the uniform and dense decoration of such surfaces with electrodeposited, microscopic, metallic electrocatalysts. Poorly controlled uniformity and spatial dispersion of electrodeposited, metallic electrocatalysts on semiconductor surfaces can be detrimental to the use of such modified semiconductors in photoelectrochemical systems, where charge-carrier recombination at the semiconductor surface depends critically on the size and spacing of metallic clusters.[70,71] Interestingly, Takabayashi et al. reported significant differences in catalyst dispersion on n-Si(111) photoelectrodes modified with different alkyl surface moieties.[34] Irregular catalyst dispersion and low resultant energy-conversion efficiencies were reported with n-Si photoelectrodes modified by linear alkyl groups. We are currently exploring the use of unsaturated organic surface groups to provide ample sites for catalyst attachment while simultaneously controlling the underlying electrical surface passivation properties.[72]

Conclusions

Significant differences were observed between the electrochemical and electrical properties of Schottky barriers formed on H- and CH_3-terminated Si(111) surfaces. Cyclic voltammetric data on the Pb or Cd electrodeposition processes on such surfaces were consistent with previous observations that the band-edge energetics in aqueous acidic solution of H-terminated n-Si(111) are offset from those of CH_3-terminated n-Si(111) by several tenths of a volt. The electrochemical observations are also in accord with prior UV photoelectron spectroscopic measurements that have elucidated the differences in interfacial dipole magnitude between the H-Si(111) and CH_3–Si(111) surfaces. The dark *J-V* responses of electrodeposited Cd and Pb films clearly exhibited more rectifying behavior on n-type CH_3–Si(111) surfaces than on n-type H-Si(111) surfaces. Chronoamperometric data on n^+-Si(111) substrates has quantitatively indicated that nucleation events during electrodeposition are an order of magnitude lower on CH_3–Si(111) surfaces than on H-Si(111) surfaces. The electrochemical and electrical properties of the electrodeposited Si(111) Schottky barriers reported herein complement previous studies on CH_3-terminated Si(111) surfaces and further emphasize the durable, well-defined, and unique electrochemical, electrical, chemical, and electronic properties of these interfaces.

Acknowledgments

We thank the National Science Foundation (Grant CHE-0604894) for financial support and the Gordon and Betty Moore Foundation for postdoctoral fellowship support (S.M.).

California Institute of Technology assisted in meeting the publication costs of this article.

References

1. P. W. Loscutoff and S. F. Bent, *Annu. Rev. Phys. Chem.*, **57**, 467 (2006).
2. A. G. Aberle, *Prog. Photovoltaics*, **8**, 473 (2000).
3. Y. J. Chabal and K. Raghavachari, *Surf. Sci.*, **502**, 41 (2002).
4. R. Cohen, L. Kronik, A. Shanzer, D. Cahen, A. Liu, Y. Rosenwaks, J. K. Lorenz, and A. B. Ellis, *J. Am. Chem. Soc.*, **121**, 10545 (1999).
5. J. M. Buriak, *Chem. Rev. (Washington, D.C.)*, **102**, 1271 (2002).
6. J. S. Hovis, S. Lee, H. B. Liu, and R. J. Hamers, *J. Vac. Sci. Technol. B*, **15**, 1153 (1997).
7. R. Boukherroub, S. Morin, F. Bensebaa, and D. D. M. Wayner, *Langmuir*, **15**, 3831 (1999).
8. T. K. Mischki, R. L. Donkers, B. J. Eves, G. P. Lopinski, and D. D. M. Wayner, *Langmuir*, **22**, 8359 (2006).
9. A. Bansal, X. L. Li, S. I. Yi, W. H. Weinberg, and N. S. Lewis, *J. Phys. Chem. B*, **105**, 10266 (2001).
10. W. J. Royea, A. Juang, and N. S. Lewis, *Appl. Phys. Lett.*, **77**, 1988 (2000).
11. T. W. Hamann and N. S. Lewis, *J. Phys. Chem. B*, **110**, 22291 (2006).
12. R. Hunger, R. Fritsche, B. Jaeckel, W. Jaegermann, L. J. Webb, and N. S. Lewis, *Phys. Rev. B*, **72**, 045317 (2005).
13. S. Maldonado, K. E. Plass, D. Knapp, and N. S. Lewis, *J. Phys. Chem. C*, **111**, 17690 (2007).
14. E. H. Rhoderick and R. H. Williams, *Metal-Semiconductor Contacts*, Clarendon Press, Oxford (1988).
15. A. Salomon, T. Boecking, O. Seitz, T. Markus, F. Amy, C. Chan, W. Zhao, D. Cahen, and A. Kahn, *Adv. Mater. (Weinheim, Ger.)*, **19**, 445 (2007).
16. Y. J. Liu and H. Z. Yu, *ChemPhysChem*, **4**, 335 (2003).
17. R. Hunger, R. Fritsche, B. Jaeckel, L. J. Webb, W. Jaegermann, and N. S. Lewis, *Surf. Sci.*, **601**, 2896 (2007).
18. M. L. Munford, F. Maroun, R. Cortes, P. Allongue, and A. A. Pasa, *Surf. Sci.*, **537**, 95 (2003).
19. K. Marquez, G. Staikov, and J. W. Schultze, *Electrochim. Acta*, **48**, 875 (2003).
20. J. M. DeLucca, S. E. Mohney, F. D. Auret, and S. A. Goodman, *J. Appl. Phys.*, **88**, 2593 (2000).
21. M. E. Kiziroglou, A. A. Zhukov, M. Abdelsalam, X. L. Li, P. A. J. de Groot, P. N. Bartlett, and C. H. de Groot, *IEEE Trans. Magn.*, **41**, 2639 (2005).
22. P. M. Vereecken, K. Rodbell, C. X. Ji, and P. C. Searson, *Appl. Phys. Lett.*, **86**, 121916 (2005).
23. G. Oskam, D. Vanmaekelbergh, and J. J. Kelly, *Electrochim. Acta*, **38**, 1115 (1993).
24. K. Ghosh and N. K. D. Chowdhury, *Int. J. Electron.*, **54**, 615 (1983).
25. Y. L. Kawamura, T. Sakka, and Y. H. Ogata, *J. Electrochem. Soc.*, **152**, C701 (2005).
26. B. Rashkova, B. Guel, R. T. Potzschke, G. Staikov, and W. J. Lorenz, *Electrochim. Acta*, **43**, 3021 (1998).
27. J. C. Ziegler, A. Reitzle, O. Bunk, J. Zegenhagen, and D. M. Kolb, *Electrochim. Acta*, **45**, 4599 (2000).
28. J. C. Ziegler, R. I. Wielgosz, and D. M. Kolb, *Electrochim. Acta*, **45**, 827 (1999).
29. R. Krumm, B. Guel, C. Schmitz, and G. Staikov, *Electrochim. Acta*, **45**, 3255 (2000).
30. P. Bindra, H. Gerischer, and D. M. Kolb, *J. Electrochem. Soc.*, **124**, 1012 (1977).
31. E. Aharonshalom and A. Heller, *J. Electrochem. Soc.*, **129**, 2865 (1982).
32. A. Heller and R. G. Vadimsky, *Phys. Rev. Lett.*, **46**, 1153 (1981).
33. S. Yae, M. Kitagaki, T. Hagihara, Y. Miyoshi, H. Matsuda, B. A. Parkinson, and Y. Nakato, *Electrochim. Acta*, **47**, 345 (2001).
34. S. Takabayashi, M. Ohashi, K. Mashima, Y. Liu, S. Yamazaki, and Y. Nakato, *Langmuir*, **21**, 8832 (2005).
35. S. U. M. Khan and J. O. Bockris, *J. Phys. Chem.*, **88**, 2504 (1984).
36. T. Zambelli, M. L. Munford, F. Pillier, M. C. Bernard, and P. Allongue, *J. Electrochem. Soc.*, **148**, C614 (2001).
37. R. M. Stiger, S. Gorer, B. Craft, and R. M. Penner, *Langmuir*, **15**, 790 (1999).
38. P. Jakob, Y. J. Chabal, K. Kuhnke, and S. B. Christman, *Surf. Sci.*, **302**, 49 (1994).
39. P. Dumas, Y. J. Chabal, R. Gunther, A. T. Ibrahimi, and Y. Petroff, *Prog. Surf. Sci.*, **48**, 313 (1995).
40. C. P. Wade and C. E. D. Chidsey, *Appl. Phys. Lett.*, **71**, 1679 (1997).
41. H. Fukidome and M. Matsumura, *Appl. Surf. Sci.*, **130–132**, 146 (1998).
42. P. Allongue, V. Kielingb, and H. Gerischer, *Electrochim. Acta*, **40**, 1353 (1995).
43. A. Bansal, X. L. Li, I. Lauermann, N. S. Lewis, S. I. Yi, and W. H. Weinberg, *J. Am. Chem. Soc.*, **118**, 7225 (1996).
44. G. Oskam, D. van Heerden, and P. C. Searson, *Appl. Phys. Lett.*, **73**, 3241 (1998).
45. G. Holmbom and B. E. Jacobson, *J. Electrochem. Soc.*, **135**, 2720 (1988).
46. K. M. S. Youssef, C. C. Koch, and P. S. Fedkiw, *J. Electrochem. Soc.*, **151**, C103 (2004).
47. M. S. Chandrasekar and M. Pushpavanam, *Electrochim. Acta*, **53**, 3313 (2008).
48. G. Oskam, J. G. Long, A. Natarajan, and P. C. Searson, *J. Phys. D*, **31**, 1927 (1998).
49. J. A. Haber and N. S. Lewis, *J. Phys. Chem. B*, **106**, 3639 (2002).
50. G. Gunawardena, G. Hills, and I. Montenegro, *J. Electroanal. Chem. Interfacial Electrochem.*, **184**, 371 (1985).
51. S. M. Sze, *Physics of Semiconductor Devices*, John Wiley & Sons, New York (1981).
52. M. X. Tan and N. S. Lewis, *Inorg. Chim. Acta*, **242**, 311 (1996).
53. M. A. Schneeweiss, H. Hagenstrom, M. J. Esplandiu, and D. M. Kolb, *Appl. Phys. A*, **69**, 537 (1999).
54. G. J. Hills, D. J. Schiffrin, and J. Thompson, *Electrochim. Acta*, **19**, 671 (1974).
55. G. Oskam and P. C. Searson, *Surf. Sci.*, **446**, 103 (2000).
56. W. Monch, *Phys. Status Solidi A*, **159**, 25 (1997).
57. S. Maldonado, D. Knapp, and N. S. Lewis, *J. Am. Chem. Soc.*, **130**, 3300 (2008).
58. X. G. Zhang, *Electrochemistry of Silicon and Its Oxide*, p. 45, Kluwer Academic/Plenum Publishers, New York (2001).
59. Unpublished results.
60. P. G. Santangelo, G. M. Miskelly, and N. S. Lewis, *J. Phys. Chem.*, **93**, 6128 (1989).
61. P. G. Santangelo, G. M. Miskelly, and N. S. Lewis, *J. Phys. Chem.*, **92**, 6359 (1988).
62. P. G. Santangelo, M. Lieberman, and N. S. Lewis, *J. Phys. Chem. B*, **102**, 4731 (1998).
63. S. R. Morrison, *Electrochemistry at Semiconductor and Oxidized Metal Electrodes*, Springer, New York (1980).
64. P. Allongue, E. Souteyrand, and L. Allemand, *J. Electroanal. Chem.*, **362**, 89 (1993).
65. H. B. Yu, L. J. Webb, R. S. Ries, S. D. Solares, W. A. Goddard, J. R. Heath, and N. S. Lewis, *J. Phys. Chem. B*, **109**, 671 (2005).
66. F. Gloaguenb, J. M. Légerb, C. Lamyb, A. Marmanna, U. Stimming, and R. Vogel, *Electrochim. Acta*, **44**, 1805 (1999).
67. R. M. Penner, *J. Phys. Chem. B*, **105**, 8672 (2001).
68. H. Liu and R. M. Penner, *J. Phys. Chem. B*, **104**, 9131 (2000).
69. P. Allongue and F. Maroun, *J. Phys. Condens. Matter*, **18**, S97 (2006).
70. R. C. Rossi, M. X. Tan, and N. S. Lewis, *Appl. Phys. Lett.*, **77**, 2698 (2000).
71. R. C. Rossi and N. S. Lewis, *J. Phys. Chem. B*, **105**, 12303 (2001).
72. K. E. Plass, X. Liu, B. S. Brunschwig, and N. S. Lewis, *Chem. Mater.*, **20**, 2228 (2008).